Effects of Ocean Climate on Spatiotemporal Variation in Sea Urchin Settlement and Recruitment

Daniel K. Okamoto*[1,2], Stephen Schroeter†[3], and Daniel C. Reed‡[3]

[1]Department of Biological Science, Florida State University, Tallahassee, Florida 32303
[2]Ecology, Evolution and Marine Biology, University of California Santa Barbara, Santa Barbara, CA 93106 USA
[3]Marine Science Institute, University of California Santa Barbara, Santa Barbara, CA 93106 USA

*corresponding author: dokamoto@bio.fsu.edu
†email: schroete@lifesci.ucsb.edu
‡email: dan.reed@lifesci.ucsb.edu

Abstract

Sea urchins are voracious herbivores that influence the ecological structure and function of nearshore ecosystems throughout the world. Like many species that produce planktonic larvae, their recruitment is thought to be particularly sensitive to climatic fluctuations in temperature that directly or indirectly affect adult reproduction and larval transport and survival. Yet how climate alters sea urchin populations in space and time by modifying larval recruitment and year-class strength on the time-scales that regulate populations remains understudied. Using an unprecedented, spatially replicated weekly-biweekly dataset spanning 27 years and 1100 km of coastline, we characterized seasonal, interannual, and spatial patterns of larval settlement of the purple sea urchin (*Strongylocentrotus purpuratus*). We show that large spatial differences in temporal patterns of larval settlement were associated with different responses to fluctuations in ocean temperature and climate. Importantly, we found a strong correlation between larval settlement and regional year class strength suggesting that such temporal and spatial variation in settlement plays an important role in controlling population dynamics. These results provide strong evidence over extensive temporal and spatial domains that climatic fluctuations shape broad-scale patterns of larval settlement and subsequent population structure of an important marine herbivore known to control the productivity and function of marine ecosystems.

Introduction

Large scale climate oscillations (e.g., El Niño/Southern Oscillation, North Atlantic Oscillation) lead to changes in ocean temperature, biogeochemistry and the severity and frequency of disruptive events that affect ocean circulation, upwelling and primary productivity (Cai *et al.* 2014; Mantua *et al.* 1997). Such shifts impose wide-reaching ecological impacts, in part by altering animal recruitment and food web structure in space and time (Sydeman *et al.* 2015). Hence, understanding how climate variability alters the recruitment of marine species is particularly important for effective conservation and management of the ocean's resources. Yet for recruitment variability, climatic fluctuations give rise to shifts in numerous factors that shape both adult reproduction and larval supply, including primary productivity, temperature, and advection and transport. Thus, significant challenges remain in achieving such understanding for benthic species with planktonic larvae due to the substantial effort needed to characterize spatial and temporal variation in larval settlement and the numerous sensitive vital rates that contribute to it.

For benthic species like sea urchins, understanding causes and consequences of recruitment variability has both ecological and economic implications. Sea urchin grazing can alter the structure of some of the world's most diverse and productive marine ecosystems, including coral reefs (Edmunds & Carpenter 2001), seagrass meadows (reviewed by Valentine & Heck Jr 1999) and kelp forests (reviewed by Filbee-Dexter & Scheibling 2014). In addition, sea urchins form the basis of important nearshore fisheries in many regions of the world (e.g. Andrew *et al.* 2003; Kato & Schroeter 1985). As a result, climate-driven changes in sea urchin

41 populations have the potential to profoundly affect the functioning of marine ecosystems and
42 the economic value of the fisheries that they support. Much of the research on controls of sea
43 urchin population dynamics has focused on the roles of predation and disease in controlling
44 adult abundance and their cascading influence on community structure (e.g. Burt *et al.* 2018;
45 Estes & Duggins 1995; Filbee-Dexter & Scheibling 2014; Lafferty 2004). Yet short-term
46 empirical studies (months to a few years) suggest that environmentally regulated larval supply
47 is likely an important driver of adult urchin dynamics (Hernández *et al.* 2010; Ling *et al.* 2009).
48 Despite the widespread recognition of the importance of recruitment variation in controlling
49 population fluctuations in many marine species (Shelton & Mangel 2011), relatively few studies
50 have examined the biotic and abiotic processes controlling the supply of sea urchin larvae in
51 nature (but see Hernández *et al.* 2010; Ling *et al.* 2009), and the degree to which they affect the
52 abundance and dynamics of older life stages over time scales that impact population dynamics.
53
54 Fluctuations in climate can affect spatial and temporal patterns of larval supply by
55 influencing the production of larvae by benthic adults, transport of larvae to adjacent habitats,
56 and the survival of larvae in the plankton. Increases in ocean temperature can impact larval
57 production by: (1) increasing adult mortality via the spread of water-borne pathogens
58 (reviewed by Feehan & Scheibling 2014), and (2) reducing adult fecundity and inhibiting
59 gametogenesis by altering food quantity and quality (Basch & Tegner 2007; Cochran &
60 Engelmann 1975; Foster *et al.* 2015; Okamoto 2014). Because sea urchins produce feeding
61 larvae that spend weeks to months in the plankton, increases in ocean temperature can also
62 affect larval development, growth and survival, either directly, or indirectly by altering the

availability of their phytoplankton food source (Bertram & Strathmann 1998; Byrne *et al.* 2009; Hoegh-Guldberg & Pearse 1995; Strathmann 1987). Finally, climate related changes in patterns of ocean circulation can affect the transport of larvae from source to destination (but see Morgan 2014; Siegel *et al.* 2008). Thus, the effects of climatic change on sea urchin recruitment represent cumulative impacts on adult abundance and reproduction, complex current patterns that transport larvae, behavioral responses of larvae, and larval development and survival. Because patterns of ocean temperature, circulation and upwelling can vary dramatically in space, the effects of climate oscillations on sea urchin recruitment potentially vary over large spatial scales. A dearth of long-term, high frequency, spatially extensive data has prevented characterizing temporal and spatial variability in larval settlement in sea urchins, the degree to which it is explained by different sources of environmental variation, and the relative importance of these drivers in accounting for fluctuations in population size.

Here we analyzed a unique 27-year weekly to biweekly time series of the recruitment of newly metamorphosed larvae (hereafter referred to as larval settlement) at sites distributed across 1100 km of coast in California to investigate sources of spatial and temporal variability in larval settlement of the purple sea urchin *Strongylocentrotus purpuratus*. Our objectives were to: (1) quantify variation in larval settlement across different temporal and spatial scales; (2) evaluate whether larval settlement on artificial substrates predicts year-class strength in natural populations; and (3) determine the relative importance of adult abundance, larval and adult food supply, sea surface temperature and broad-scale fluctuations in ocean climate in contributing to the observed variation in larval settlement

85 ***Study system***

86 Populations of the purple sea urchin (*Strongylocentrotus purpuratus*) occupy shallow
87 subtidal and intertidal rocky substrata from at least 27°N on the western coast of the Baja
88 Peninsula (Olivares-Bañuelos *et al.* 2008) to at least 59°N on the Kenai Peninsula in Alaska (Field
89 & Walker 2003). Purple urchins are broadcast spawners and the seasonality of their spawning
90 is generally thought to be driven by spring photoperiod and temperature (Cochran &
91 Engelmann 1975; Gonor 1973; Pearse *et al.* 1986). Results from the field and laboratory
92 indicate that the thermal upper limit to completion of gametogenesis may lie around 17°C
93 (Basch & Tegner 2007; Cochran & Engelmann 1975). Fertilized zygotes develop into planktonic
94 echinoplutei larvae that feed exclusively on phytoplankton (Strathmann 1987). After spending
95 several weeks to months in the plankton, individuals begin final metamorphosis and settle to
96 the benthos (Strathmann 1978) at a size of ~500 μm in diameter (Okamoto unpublished data).
97 Larval settlement varies dramatically among locations at both small and large spatial scales
98 (Ebert 2010). Once settled, fully competent individuals occupy cobble and other complex
99 substrata and between 12-24 months become visible in benthic surveys at 1-2 cm diameter.
100

101 ***Collection of newly settled urchins along the coast of California, USA (1990-2016)***

102 Settlement of newly metamorphosed purple sea urchins was sampled in three major
103 regions along the California coast from 1990 through 2016, with a total of 54,588 replicate
104 observations. Sampling regions (from south to north) included two sites in San Diego County
105 (Scripps Pier and Ocean Beach Pier), four sites in the Santa Barbara Channel (Anacapa Island,
106 Stearns Wharf, Ellwood Pier and Gaviota Pier) and one site at Point Cabrillo in Fort Bragg (Figure

1). San Diego and the Santa Barbara Channel lie within the Southern California Bight and Fort Bragg is in northern California. At each site, newly settled urchins were collected using nylon-bristled scrub brushes (2.5 cm long bristles and a 6 x 9 cm wooden base) suspended 1 to 2 m from the benthos (Ebert *et al.* 1994). The majority of deployments included 4-8 replicate brushes collected weekly at each site from 1990 to 2003, and biweekly thereafter through 2016. Upon collection brushes were transported to the laboratory in plastic bags and rinsed through a 350 μm mesh sieve. Purple urchins were sorted from other species, counted and preserved. See (Ebert *et al.* 1994) for further details.

Methods

Spatio-temporal trends in larval settlement

We estimated seasonal, annual, and spatial patterns in larval settlement using an integrated spatiotemporal Bayesian model that accounted for the spatially and temporally intercorrelated and heterogeneous nature of the multivariate time series. We used a Bayesian state-space formulation for the model for several reasons. First, episodic periods of low replication, low observation numbers, missing data, or slight variation in the sampling interval mean that the true number of settlers may not be reflected in the empirical mean value from brush data (i.e. the true value is not always observable). Second, when brushes contained hundreds or more individual urchins, species identification consisted of subsampling urchins to estimate proportions of individual species (in this case *S. purpuratus* versus the more rare red urchin, *Mesocentrotus franciscanus*). This subsampling routine requires accounting for the uncertainty in the sampled species ratios in the estimation of settler abundance, which we did

by incorporating a Bayesian prior in the form of a Beta distribution with hyperparameters as the observed ratio and total subsample count (the Jeffrey's prior for ratios from binomial counts). Third, initial examination of the data indicated that there were strong temporal components (interannual and seasonal trends, substantial and multiplicative among-sample variability within each period, and serial autocorrelation) and spatial components that needed to be simultaneously accounted for.

To account for the above described nuances of the data we estimated biweekly settlement density ($\hat{\mu}_{t,l}$) as the sum of a site-specific mean ($\beta_{0,l}$), log annual trend ($\mathrm{Annual_Trend}_{s,t}$), log seasonal trend ($\mathrm{Seas_Trend}_{t,l}$), and a spatially correlated lognormal process error ($\varepsilon_{t,l}$);

Eq. 1 $\ln\ \hat{\mu}_{t,l} = \beta_{0,l} + \ln \mathrm{Annual_Trend}_{t,l} + \ln \mathrm{Seasonal_Trend}_{t,l} + \varepsilon_{t,l}$ (Trend Equation)

We estimated trends on the log-scale so that process errors, and seasonal and interannual trends were multiplicative and strictly positive on the original scale. We used a Poisson observation likelihood to link the biweekly mean estimate from the trend equation ($\hat{\mu}_{t,l}$ -see Tables 1 and 2) to observed counts of larval settlers (N) for each brush (b) within each site within each year .

The annual trends were assumed to be correlated in both space and time, where spatial and temporal covariances were assumed to be independent. The annual spatial covariance was assumed to be unstructured (i.e. no formal distance decay structure) because we only had seven sites. The annual temporal covariance was determined by a Matérn 3/2 kernel because it provided sufficient flexibility to capture interannual trends. The seasonal trend (log-scale)

within each site was estimated using a seasonal periodic temporal kernel within the model to capture the cyclical nature of seasonality. The process error ($\varepsilon_{t,l}$) was modeled with an unstructured spatial covariance to account for correlations among sites in their deviations from model expectations. We estimated the model posteriors using Stan (Carpenter *et al.* 2016) with three 1000 iteration chains after a 1000 iteration burn-in. Stan model code is provided in the supplement. For model equations and symbology see Tables 1 and 2.

Relationship between benthic year-class strength and larval settlement.

If year class strength of sea urchins is limited by larval supply, then we should see increases (decreases) in the abundance of juveniles in years following anomalously high (low) larval settlement. We therefore tested whether larval settlement in the Santa Barbara Channel (mean of Anacapa, Stearns Wharf, Ellwood Pier and Gaviota Pier) was predictive of subsequent juvenile recruitment (hereafter referred to as "year-class strength") on natural reefs in the region. We calculated densities of juveniles (<2cm test diameter) from the Channel Islands Kelp Forest Monitoring (KFM) Program (Kushner *et al.* 2013), including only the XXX sites with time series extending from 1990 through 2016. We examined the relationship between larval settlement and year-class strength using a generalized linear mixed effects model (GLMM) with a negative binomial likelihood (a Poisson likelihood indicated overdispersion) and survey site as a random effect. We tested the hypothesis of no correlation using a likelihood ratio test comparing the model with versus without settlement as a covariate. Models were estimated using glmmTMB (Magnusson *et al.* 2017) in R (see Electronic Supplement for further details).

Relationships between larval settlement and biotic and abiotic conditions

We estimated the strength of relationships between biweekly larval settlement and various hypothesized physical and biological drivers using an integrated regression model that included a regularized regression within a Bayesian time-series modelling framework (Fig. 2). Specifically, the model considered estimated log biweekly density ($\ln \hat{\mu}_{t,l}$) as a function of the centered and standardized covariates (denoted by the vector $\boldsymbol{x_{t,l}}$) while directly estimating and accounting for seasonal trends ($\mathrm{Seasonal_Trend}_{t,l}$), and separable spatially and temporally correlated, multivariate lognormal process error ($\varepsilon_{t,l}$):

Eq. 2 $$\ln \hat{\mu}_{t,l} = \beta_{0,l} + \left[\boldsymbol{x_{t,l}}\right]'\boldsymbol{\beta_l} + \ln \mathrm{Seasonal_Trend}_{t,l} + \varepsilon_{t,l}$$ (Regression Equation)

We used a Poisson observation likelihood to link the latent trends $\hat{\mu}_{t,l}$ to the observations (see Tables 1, 2) and we assumed the temporal correlation in the process error followed a first order autoregressive model.

Because these analyses were correlative, we focused on unbiased parameter estimation rather than hypothesis testing or model comparison per se. We estimated two separate models: one included all locally measured (i.e. for a given site) environmental variables and the other included a common set of composite indices of oceanographic climate ("global covariates" – ENSO Index, Pacific Decadal Oscillation, North Pacific Gyre). Because inclusion of numerous covariates can cause overfitting that leads to bias and uncertainty in the explanatory power of the covariates, we erred on the side of sparsity and assigned the vector of regression coefficients ($\boldsymbol{\beta_l}$) a regularized horseshoe prior (i.e. the Finnish Horseshoe). Sparsity in this case

assumed that only a few of the covariates were meaningful without a priori knowledge of which covariates were relevant and which were not. A sparse regression encoded this assumption to allow the data to inform which covariates were relevant and how they were correlated with the response variable. The Finnish horseshoe prior is a Bayesian version of the lasso (Carvalho *et al.* 2010; Piironen & Vehtari 2017) that produced a data-driven reduction in the influence of weaker covariates by regularization of those coefficients given the data. For full details and model equations, see Tables S.1 and S.2.

Below are the covariates used in the integrated regression model:

(i) Oceanographic climate indices (monthly, 1990-2016, all sites): We used three major global indices of oceanographic climate. The multivariate El Niño Southern Oscillation Index (MEI), the Pacific Decadal Oscillation (PDO - Mantua & Hare 2002) and the North Pacific Gyre Oscillation (NPGO - Di Lorenzo *et al.* 2008). The MEI provides a metric of the intensity of El Niño Southern Oscillation (ENSO) fluctuations, which persist for 6-18 months and explains much of the oceanographic variability in the tropics (Di Lorenzo *et al.* 2013; Wolter & Timlin 1993; Wolter & Timlin 1998). In contrast, the PDO and NPGO exhibit longer-period fluctuations, explain much of the oceanographic variability in higher latitudes, and the low frequency variability of these metrics are shaped through ENSO forcing of the Aleutian Low and the North Pacific Oscillation, respectively (Di Lorenzo *et al.* 2013).

214 *(ii) Coastal upwelling index (monthly, 1997-2016, all sites):* The Bakun index (Bakun
215 1973) provides an index of large-scale coastal upwelling and specifically describes the volume of
216 water that is transported offshore from Ekman transport (http://www.pfel.noaa.gov/ - sites =
217 33N-119W and 39N-125W. This index has been used as a large-scale proxy for processes that
218 may favor larval retention and advection from shore in addition to its value as a predictor of
219 coastal productivity (Menge *et al.* 2011; Menge & Menge 2013; Shkedy & Roughgarden 1997;
220 Wing *et al.* 2003). We emphasize that this index is not a location specific metric nor does it
221 consider fine-scale nearshore hydrodynamic processes that are also likely to affect larval
222 retention (Fisher *et al.* 2014; Morgan *et al.* 2009; Morgan *et al.* 2016; Morgan *et al.* 2018;
223 Shanks & Shearman 2009; Shanks & Eckert 2005; Shanks & Morgan 2018; Shanks *et al.* 2017)
224 which remain outside the scope of this study but worthy of investigation as drivers of
225 settlement trends. Rather we include the Bakun index here as an index of broader scale coastal
226 upwelling that some argue affect trends in larval supply.
227
228 *(iii) Sea surface chlorophyll (monthly, 1997-2016, all sites)*: Satellite imagery of sea
229 surface chlorophyll a provides a spatially and temporally resolved estimate of phytoplankton
230 biomass (mg m^{-3}) that is not available from in situ sampling. We used version 3.1 of the OC-CCI
231 merged ocean color time series (Sathyendranath *et al.* 2018) that combines SeaWIFs, MERIS,
232 MODIS and VIIRS to provide the temporal and spatial coverage required for this study. For each
233 larval settlement collection site, we aggregated data into a 30-day moving average (30 days
234 prior to brush collection) within a buffer of 10 km from shore that stretched 150 km alongshore
235 (the average Lagrangian estimate for dispersal distances for species with a planktonic larval

236 duration (PLD) of 30-days (but see Shanks 2009; Siegel *et al.* 2003)). For the site at Anacapa
237 Island, we included any point within a 150 km radius and within 10 km of any coastline. We
238 used 30-day moving averages for chlorophyll and temperature (below) because larvae were
239 exposed to these conditions for at least 30 days prior to settlement, and because averaging
240 over 30 days minimized the effects of serial autocorrelation in the data.
241
242 (*iv) Sea surface temperature (monthly, 1997-2016, all sites):* We used the 30-day moving
243 average of sea surface temperature, derived from Pathfinder AVHRR (Reynolds *et al.* 2007)
244 (advanced very high resolution radiometer) that was optimally interpolated at daily and 0.25
245 degree latitude/longitude resolution. We spatially aggregated data in the same way as sea
246 surface chlorophyll.
247
248 *(v) Fall kelp canopy biomass (annual, 1996-2015, Santa Barbara Channel & San Diego*
249 *only):* Giant kelp (*Macrocystis pyrifera*) is a preferred food and a major constituent of *S.*
250 *purpuratus* diets in southern California (Harrold & Reed 1985). The regional biomass of giant
251 kelp *Macrocystis pyrifera* can fluctuate dramatically from year to year (Bell *et al.* 2015) and
252 cause orders of magnitude variations in *S. purpuratus* fecundity (Okamoto 2014). We estimated
253 intra and interannual variability in the biomass of giant kelp from Landsat Thematic Mapper
254 satellite imagery (Bell 2017). Data were aggregated for the Santa Barbara Channel (including
255 islands and mainland from Point Conception to Santa Monica Bay through Ventura County) or
256 the San Diego region (mainland coast from the US-Mexico through Orange County including
257 Santa Catalina and San Clemente Islands). We used the 3-month running mean of kelp canopy

biomass during the period leading into the spawning season (Sept-Nov) because marked declines in reproductive capacity require several months of consistently low food supply (Okamoto 2014).

(vi) Adult sea urchin density in the Channel Islands (annual, 1997-2016, Santa Barbara Channel only): The abundance of adult sea urchins can also fluctuate over time, which can affect larval production and supply. We used the spatial geometric mean of adult biomass density (kg m^{-2}) of purple sea urchins (calculated from surveys of density and size structure from the Channel Islands Kelp Forest Monitoring program and a size-biomass model from the Santa Barbara Coastal LTER) as an index of the density of adult purple sea urchins in the Santa Barbara Channel. We used the geometric mean (exponentiated log-scale mean) as it accounts for spatial differences in overall mean abundance among sites. We use a biomass index that incorporates size structure and density instead of justdensity because individual maximum fecundity increases with size. For details on calculation of biomass from the KFM data see the Electronic Supplement.

We allowed regression coefficients to vary among major regions (Fort Bragg, Santa Barbara, and San Diego sites). We used this level of inference because the covariates are aggregated over spatial regions that encompass all sites within a region due to the long planktonic larval duration of sea urchins. The regression analyses included either all global covariates (ENSO, PDO, NPGO) or all local covariates (temperature, chlorophyll, adult densities, giant kelp biomass, and the Bakun upwelling index). We conducted separate analyses for these

two groups of covariates because global indices were directly correlated with local covariates, or in the case of temperature were partially derived from them. Thus, our analyses provided non-mechanistic explanatory variables for global covariates and mechanistic explanatory variables for local covariates.

Results

Spatio-temporal trends in larval settlement

Substantial interannual variability in larval settlement of *S. purpuratus* was observed among years (Figure 3, Appendix Figure S1). Fluctuations in larval settlement were highly synchronous among sites within each of the two regions in the Southern California Bight (r = 0.73 and 0.85 for sites within the Santa Barbara Channel and San Diego, respectively; Figure 3b, c). Within the Santa Barbara Channel, pairwise correlations in interannual trends involving Gaviota, Ellwood and Stearns Wharf were higher (r =0.86 to 0.90) than those involving Anacapa (r = 0.46 to 0.71). Anacapa began to decline in 2012, while the declines at the other sites did not begin until 2014 (Figure 3b, Appendix Figure S.1 b-e). While all of the Santa Barbara Channel sites except Anacapa exhibited eight continuous years of above average settlement following the low in 2005, San Diego sites remained mostly below average after 2003(Figure 3c, Appendix Figure S.1 f-g). This trend produced modest synchrony among San Diego and Santa Barbara sites from 1991 through 2007 (mean r = 0.68), but none thereafter (mean r= -0.06). In contrast, interannual trends in larval settlement at Fort Bragg were largely uncorrelated throughout the time series with sites in the Santa Barbara Channel (Figure 3a vs. 3b, mean r = -0.23) and sites in San Diego (Figure 3a vs. 3c; mean r = 0.12).

Larval settlement in southern California (San Diego and the Santa Barbara Channel) was highly seasonal, with similar patterns among sites (Figure 4, Appendix Figure S2). On average 90% of recruitment occurred from March to July with a single peak in late April/early May (Figure 4a). By contrast, recruitment at Fort Bragg in northern California extended over a longer period of time (90% occurred, between January and September) and typically included two peaks per year (a large peak around July and a smaller peak in February and March; Figure 4a). The seasonal peaks in settlement in southern California coincided with peaks in sea surface chlorophyll (Figure 4a vs. 4b.) and troughs in sea surface temperature (Figure 4a vs. 4c). At Fort Bragg in northern California the primary peak occurred slightly after the peak in chlorophyll a (Figure 4a. vs. 4b).

Relationship between benthic year-class strength and larval settlement.

Recruitment of juvenile purple urchins at shallow subtidal reefs in the Santa Barbara Channel exhibited a significant, positive correlation with larval settlement to brushes two years prior (Figure 5**,** negative binomial GLMM - $\chi^2_{\mathrm{df}=1}$= 9.48, p = 0.002). Years with the highest larval settlement corresponded with a nearly three-fold increase in the mean density of juvenile urchins two summers later (Figure 5). Over the time series, average settlement densities in the Santa Barbara Channel varied by more than three orders of magnitude among years. This interannual variation in settlement (averaged across the sites in the Santa Barbara Channel) corresponded to, on average, more than a three-fold increase in the density of benthic juveniles.

Relationships between larval settlement and biotic and abiotic conditions

Larval settlement of purple urchins showed strong correlations with local sea surface temperature (SST, Figure 6 a-g, Figure 7 a) as well as the major climate indices (e.g. ENSO - Fig 6 h-n, Figure 7f). For temperature and ENSO, the sign of the correlation at Fort Bragg was opposite of that at sites in the Santa Barbara Channel and San Diego. The correlation between settlement and temperature varied from strongly negative at sites in San Diego and Santa Barbara to positive at the Fort Bragg site. Correlations between larval settlement and adult urchin density, upwelling, chlorophyll and kelp biomass were either not different from zero or were opposite of that expected at all sites (Figure 7 b-e). Larval settlement and sea surface chlorophyll were uncorrelated at Fort Bragg and in the Santa Barbara Channel and negatively correlated in San Diego – the opposite of the hypothesized relationship that more food in the plankton would lead to higher larval settlement (Figure 7 d). The network of correlations among these variables are depicted in (Appendix Figure S.3).

Larval settlement in southern California was orders of magnitude lower during warm, El Niño conditions and during the negative phase of the NPGO with the more southern sites in San Diego responding more strongly to temperature than those further north in the Santa Barbara Channel (Figure 7 a). In contrast, Fort Bragg, the northern most site, responded positively to warmer El Niño conditions, negatively to the NPGO, and positively to the PDO. Importantly, relationships observed between larval settlement and ENSO and temperature in southern California were opposite of those observed at Fort Bragg (Figure 7 f, g). The correlations

346 between larval settlement and SST and ENSO occurred on roughly 3-5 year cycles, while the
347 correlation with NGPO and PDO occurred on decadal scales.
348

349 ## Discussion

350 Climate variability can significantly impact marine ecosystems by affecting recruitment
351 which in turn influences the dynamics of populations and communities. Yet determining which
352 species and communities will respond to shifting climate remains a difficult task. Using a multi-
353 decadal, high frequency, and spatially extensive time series we show how large-scale climatic
354 variation can give rise to spatially different responses in the settlement of larval sea urchins.
355 We found that settlement patterns were synchronous within Santa Barbara and San Diego and
356 synchronous among regions until the late 2000s. Importantly, these sites responded negatively
357 to elevated temperature and ENSO events. This contrasted sharply with settlement at our
358 northern California site (Fort Bragg) which was positively correlated to temperature and ENSO.
359 This difference was most obvious during the two strongest ENSO events in 1998 and 2014,
360 when settlement responded dramatically in opposite directions.
361

362 While many recruitment-environment correlations often break down over time (Myers
363 1998), the correlations between oceanographic factors and larval settlement in our study were
364 evident over a 27-year period that included multiple major ENSO events and several minor
365 ones. We observed repeatable patterns of diminished larval settlement in response to
366 temperature and ENSO events in southern California with opposite responses at Fort Bragg in
367 northern California. Others have found larval settlement in sea urchins to be positively or

negatively related to temperature depending on the species (Ebert 1983; Hernández *et al.* 2010) (Ebert 1983, Himmelman 1986 Hernandez et al. 2010). Our study is among the first to show that the relationship between larval settlement and temperature can vary dramatically within a species depending on location. Although sea urchin larval settlement data at the fine temporal scale of our study are not available prior to 1990, there is a history of evidence for ENSO-related recruitment failures in sea urchin populations off southern California. Between 1969 and the early 1980's, recruitment of juvenile sea urchins was anomalously low during El Niño years (Ebert 1983; Tegner & Dayton 1991). Between 1969 and 1977, juvenile recruitment was lowest during the El Niño years of 1970, 1973, and 1977 at False Point, California near San Diego (Ebert 1983; Tegner & Dayton 1991) and at nearby Point Loma, low recruitment followed the 1982-83 El Niño event (Ebert 1983; Tegner & Dayton 1991). How patterns of larval settlement change in the future will undoubtedly depend on the processes underlying their associations with ENSO events.

Climate related fluctuations in the supply of larvae have been hypothesized to affect coastal species around the world (Caley *et al.* 1996; Grosberg & Levitan 1992; Underwood & Fairweather 1989). In the case of sea urchins, larval supply has been linked to dramatic changes in the state of benthic communities (Estes & Duggins 1995; Hernández *et al.* 2010; Ling *et al.* 2009). Yet empirically demonstrating such links has historically proved challenging because recruitment can be attenuated by high mortality of newly settled larvae (Connell 1985; Rowley 1989), increasing the need for high frequency data of larval settlement spanning multiple years. Data such as ours that meet these criteria are rare.

The potential factors affecting larval supply that we examined other than temperature and climate showed no meaningful correlations with larval settlement. Of particular note was the lack of a correlation with ocean chlorophyll revealed by our analyses. This finding differed from that observed for the tropical sea urchin *Diadema aff. antillarum* (Hernández *et al.* 2010) and highlights a need for exploring mechanistically how spatial and temporal variability in ocean circulation and phytoplankton productivity affect patterns of larval settlement. Like recent studies (Shanks & Shearman 2009; Shanks & Morgan 2018), we found no relationship between large-scale fluctuations in upwelling and larval settlement, which runs counter to hypotheses that large-scale coastal upwelling shapes patterns of larval supply by broadly altering productivity and retention (Menge & Menge 2013; Roughgarden *et al.* 1991). The major ocean currents in our study system (the Southern California Counter Current and the California Current) are characterized by stochastic and spatially variable eddies, fronts, filaments and bores (e.g. Bassin *et al.* 2005; Davis *et al.* 2008; DiGiacomo & Holt 2001), whereas flows closer to shore tend to promote larval retention along wave exposed shores (Morgan *et al.* 2016; Shanks *et al.* 2017). As a result, offshore transport and retention off the coast of California is spatially nuanced and temporally inconsistent (Shanks & Eckert 2005). Such heterogeneity not only influences larval transport, but also when and where larvae encounter productive food environments. Consequently, if larval food limitation plays a role in shaping the dynamics of urchin settlement at our sites, then it likely arises out of more complex dynamics than our spatially aggregated composite metrics were able to detect. For example, processes that shape stratification, front formation and spatially isolated phytoplankton blooms

412 in combination with larval behavior may play a more important role than predicted by
413 simplifications of the higher or lower spatially averaged phytoplankton production or greater or
414 lesser coastal upwelling. Integrating quantitative measurements of these processes was
415 beyond the scope of our study, yet such approaches are needed to develop a mechanistic
416 understanding of processes that control settlement dynamics across large gradients in
417 oceanographic settings.
418
419 Although climate related changes can alter larval supply via their effects on the
420 production of larvae by adults, we found no relationship between larval settlement and
421 regional adult abundance or adult food (kelp). While fisheries research relies heavily on stock-
422 recruit dynamics, there is continual debate about whether adult dynamics actually control
423 recruitment patterns (Gilbert 1997; Szuwalski *et al.* 2015). The lack of a positive correlation
424 between adults and larval settlement that we found for purple sea urchins adds to this debate
425 by showing that high abundances of adult urchins and kelp averaged across large spatial scales
426 did not translate into high larval supply. We note that spatial structure in the dynamics of kelp
427 and adult urchins may have affected this outcome. For example, modest but uniform densities
428 of adult sea urchins in food rich kelp forests can provide very different outcomes for the
429 production of embryos compared to mosaics of dense adults in barren patches interspersed
430 with forested patches having few adults (Okamoto 2014; Okamoto 2016). Indeed, previous
431 work has demonstrated that assessing population productivity in spatially structured
432 populations requires a spatially structured analysis to account for processes of population
433 regulation and competition (Chesson 1996, 1998; Chesson *et al.* 2005; Thorson *et al.* 2015).

434 That said, we found no evidence that synchronous fluctuations in settlement arose from broad-
435 scale collapses and proliferations in populations of adult sea urchins or kelp at the appropriate
436 lags and time-scales.
437
438 Temperature-related effects on larval production and survival and ENSO-related
439 changes in currents or oceanographic features that transport larvae represent two possible
440 explanations for the spatially opposing correlations between larval settlement and temperature
441 and ENSO that we observed. Many species have upper temperature thresholds beyond which
442 reproduction is impaired that are well below the lethal limits for adults. Temperatures in
443 southern California kelp forests routinely exceed 17°C during ENSO events (Reed et al. 2016),
444 which may adversely affect larval supply of purple sea urchins by limiting gamete production
445 (Basch & Tegner 2007; Cochran & Engelmann 1975), fertilization (Schroeder & Battaglia 1985)
446 larval development and gene expression (Padilla-Gamiño *et al.* 2013; Runcie *et al.* 2012; Wong
447 *et al.* 2018), and larval survival (Azad *et al.* 2012). Such effects may in part explain why larval
448 settlement at Fort Bragg, where sea surface temperatures rarely exceed 16°C (Figure 6a) was
449 not negatively correlated with temperature.
450
451 Regional circulation is considered to be an important driver of larval supply for many
452 species, including those in the Southern California Bight (Blanchette *et al.* 2006; Broitman *et al.*
453 2005; McManus & Woodson 2012; Woodson *et al.* 2012). ENSO events can cause major
454 changes in patterns of ocean circulation along the US west coast. For example, the 1997/98 El
455 Niño caused anomalously strong poleward flow and decreased local retention in coastal areas

off southern California (Lynn & Bograd 2002; Mitarai *et al.* 2009). Yet El Niño events also create stochastic small-scale patterns of water motion in the form of fronts, eddies, and bores (Pineda *et al.* 2018). Spatial variability in such patterns could explain the opposing climatic responses in larval settlement between Fort Bragg and our sites in southern California. El Niño events in southern California are associated lower stratification and reduced internal waves that promote the onshore transport of larvae (Pineda 1994; Pineda *et al.* 2018; Shanks 1983). In contrast, El Nino events in northern California are often associated with relaxed upwelling, downwelling Kelvin waves and increased stratification (Chavez *et al.* 2002). Although we cannot definitively partition out the effects of climate associated changes in temperature and circulation on recruitment, our observations of larval settlement and subsequent year-class strength point strongly to broader-scale ocean climate effects.

Our finding that larval settlement was a good predictor of year class strength in natural populations indicates that large fluctuations in larval settlement of this prominent herbivore could have far reaching ecological impacts that resonate throughout marine ecosystems across a broad geographic region (Pearse 2006). For example, the high settlement that we observed in Fort Bragg in 2013-2015 coupled with a period of anomalously warm water may explain the marked increase in the abundance of purple urchins and coincident loss of canopy forming kelps reported for northern California beginning in 2014 (Catton *et al.* 2016). Our results suggest that predicted changes in ocean climate that lead to more frequent or severe marine heatwaves (Frölicher and Laufkötter 2018) will reduce purple urchin recruitment in southern California, but increase it in northern California with potentially cascading effects on benthic ecosystems similar to those recently observed in northern California.

Oceans are experiencing simultaneous shifts in temperature, water chemistry, productivity and circulation, which have profound consequences for the ecological structure and function of marine systems and the services that they provide (Wong *et al.* 2014). Our findings provide valuable insights into the ecological consequences of climate related effects on patterns of larval settlement of an important reef herbivore whose distribution spans most of the Pacific coast of North America. Future investigations aimed at determining the specific biotic and abiotic processes that regulate larval settlement in ecological important species such as *S. purpuratus* will undoubtedly improve our understanding of how climate fluctuations affect regional population dynamics to alter the structure and functions of marine ecosystems.

Acknowledgements

Funding was provided by the California Urchin Commission, the South Bay Cable Committee, the California Department of Fish and Wildlife Director's Sea Urchin Advisory Committee, and the National Science Foundation's support of the Santa Barbara Coastal Long Term Ecological Research program. We are indebted to Tom Ebert and John Dixon, who initiated the larval settlement time series with SS. The Channel Islands Naturalist Corps volunteers, Channel Islands National Park Staff, and Channel Islands long term Kelp Forest Monitoring Program were and remain instrumental in collecting settlement data from Anacapa and benthic data in the Channel Islands. John Richards, Clint Nelson, Shannon Harrer, Jenny Wolf, Peter Kalvass, Brigitte Bondoux and many students assisted with field collections, laboratory sampling and data compilation. Sally Holbrook, Russ Schmitt and Cherie Briggs contributed discussions during initial development of analyses. Kyle Cavanaugh, Dave Siegel and Tom Bell provided

valuable discussions about giant kelp canopy data. Kyle Cavanaugh and Rachel Simons gave important comments on previous manuscript drafts.

List of Figures

Figure 1: Map of larval settlement collection sites in California. Colors represent the average spatial gradient of sea surface temperature from 1991-2017. The hatched white lines show the shoreline buffer used to constrain sea surface temperature and sea surface chlorophyll index to local larval settlement observations.

Figure 2: Diagram of the model structure using either a Matérn temporal covariance (trend estimation model) or a horseshoe regression (correlation estimation model) to estimate seasonal anomalies. For details see Tables 1 and 2. *Bayesian Regression Model Only. †Trend Estimation Model Only

Figure 3: Standardized annual scale trends (log-scale, standardized to one SD) of larval settlement *S. purpuratus* from 1990 through 2016 for: (a) Fort Bragg, (b) sites in the Santa Barbara Channel, and (c) sites in San Diego. Colors within represent individual sites associated with the legend. Interannual trends are estimated using a 3/2 Matérn Gaussian process covariance within a Bayesian multivariate state-space model accounting for spatiotemporal correlations.

Figure 4: Seasonal trends at each site for: (a) standardized larval settlement of *S. purpuratus*, (b) biweekly mean sea surface chlorophyll a (chl a) and (c) biweekly mean sea surface temperature (SST). The seasonal trend in larval settlement at each site was standardized by the mean maximum seasonal value. Chl a and SST were measured using satellite imagery within 25 km of

the coastline and 150 alongshore km of the location where settlement was sampled (hatched areas in Figure 1). See Methods for details.

Figure 5: The relationship between the summer density of juvenile purple sea urchins on reefs in the Santa Barbara Channel and the density of recruits on larval collectors during March- July of the previous year (i.e., 12-20 months prior). Points and error bars represent annual means (+/- SE) averaged over all sites. The line with the band represents the estimated relationship and 95% uncertainty interval.

Figure 6: Standardized coefficients for the relationships between larval settlement of purple sea urchins at each site and: (a-g) sea surface temperature, (h-n) the multivariate ENSO index, and (m-u) the North Pacific Gyre Oscillation (NPGO). Small grey points represent biweekly means and black points and lines represent annual means.

Figure 7: Standardized Bayesian multiple regression coefficients for relationships between *S. purpuratus* and local covariates (a-e) or global climatic indices (f-h). Models with global and local variables were fit separately. Coefficients were estimated using a multiple regression nested within a Bayesian multivariate time series model. Coefficients are *a priori* biased towards zero using a regularized horseshoe prior for variable selection. For details see Methods.

References

Andrew N., Agatsuma Y., Ballesteros E., Bazhin A., Creaser E., Barnes D., Botsford L., Bradbury A., Campbell A. & Dixon J. (2003) Status and management of world sea urchin fisheries. *Oceanography and Marine Biology-An Annual Review*, 40, 343-425

Azad A.K., Pearce C.M. & McKinley R.S. (2012) Influence of stocking density and temperature on early development and survival of the purple sea urchin, *Strongylocentrotus purpuratus* (Stimpson, 1857). *Aquac Res*, 43, 1577-1591

Bakun A. 1973. Coastal upwelling indices, west coast of North America, 1946-71. US Department of Commerce, National Oceanic and Atmospheric Administration, National Marine Fisheries Service pp. 103.

Basch L.V. & Tegner M.J. (2007) Reproductive responses of Purple sea urchin (*Strongylocentrotus purpuratus*) populations to environmental conditions across a coastal depth gradient. *Bull Mar Sci*, 81, 255-282

Bassin C.J., Washburn L., Brzezinski M. & McPhee-Shaw E. (2005) Sub-mesoscale coastal eddies observed by high frequency radar: A new mechanism for delivering nutrients to kelp forests in the Southern California Bight. *Geophysical Research Letters*, 32

Bell T., K. Cavanaugh and D. Siegel, (2017) SBC LTER: Time series of quarterly NetCDF files of kelp biomass in the canopy from Landsat 5, 7 and 8, 1984 - 2016 (ongoing). Santa Barbara Coastal Long Term Ecological Research Project. doi:10.6073/pasta/817d2c24ebd78621869e17d94ba0df0c

Bell T.W., Cavanaugh K.C., Reed D.C. & Siegel D.A. (2015) Geographical variability in the controls of giant kelp biomass dynamics. *J Biogeogr*, 42, 2010-2021

Bertram D.F. & Strathmann R.R. (1998) Effects of maternal and larval nutrition on growth and form of planktotrophic larvae. *Ecology*, 79, 315-327

Blanchette C.A., Broitman B.R. & Gaines S.D. (2006) Intertidal community structure and oceanographic patterns around Santa Cruz Island, CA, USA. *Mar Biol*, 149, 689-701

Broitman B.R., Blanchette C.A. & Gaines S.D. (2005) Recruitment of intertidal invertebrates and oceanographic variability at Santa Cruz Island, California. *Limnol Oceanogr*, 50, 1473-1479

Burt J.M., Tinker M.T., Okamoto D.K., Demes K.W., Holmes K. & Salomon A.K. (2018) Sudden collapse of a mesopredator reveals its complementary role in mediating rocky reef regime shifts. *Proc R Soc B*, 285

Byrne M., Ho M., Selvakumaraswamy P., Nguyen H.D., Dworjanyn S.A. & Davis A.R. (2009) Temperature, but not pH, compromises sea urchin fertilization and early development under near-future climate change scenarios. *Proc R Soc B*, 276, 1883-1888

Cai W., Borlace S., Lengaigne M., Van Rensch P., Collins M., Vecchi G., Timmermann A., Santoso A., McPhaden M.J. & Wu L. (2014) Increasing frequency of extreme El Niño events due to greenhouse warming. *Nature climate change*, 4, 111

Caley M., Carr M., Hixon M., Hughes T., Jones G. & Menge B. (1996) Recruitment and the local dynamics of open marine populations. *Annu Rev Ecol Syst*, 27, 477-500

Carpenter B., Gelman A., Hoffman M., Lee D., Goodrich B., Betancourt M., Brubaker M.A., Guo J., Li P. & Riddell A. (2016) Stan: A probabilistic programming language. *J Stat Softw*, 20

Carvalho C.M., Polson N.G. & Scott J.G. (2010) The horseshoe estimator for sparse signals. *Biometrika*, 97, 465-480

Catton C., L. , Bennett R. & Amrhein. A. (2016) Perfect storm decimates northern California kelp forests. California Department of Fish and Wildlife Marine Management News. https://cdfwmarine.wordpress.com/2016/03/30/perfect-storm-decimates-kelp/

Chavez F., Pennington J., Castro C., Ryan J., Michisaki R., Schlining B., Walz P., Buck K., McFadyen A. & Collins C. (2002) Biological and chemical consequences of the 1997–1998 El Niño in central California waters. *Progress in Oceanography*, 54, 205-232

Chesson P. 1996. Matters of scale in the dynamics of populations and communities. In: *Frontiers of population ecology* (eds. RB Floyd, AW Sheppard & PJ de Barro). CSIRO, Victoria, Australia. pp. 353-368.

Chesson P. (1998) Spatial scales in the study of reef fishes: a theoretical perspective. *Aust J Ecol*, 23, 209-215

Chesson P., Donahue M.J., Melbourne B.A. & Sears A.L. 2005. Scale transition theory for understanding mechanisms in metacommunities. In: *Metacommunities: spatial dynamics and ecological communities* (eds. M Holyoak, MA Leibold & RD Holt). University of Chicago Presspp. 279-306.

Cochran R.C. & Engelmann F. (1975) Environmental regulation of the annual reproductive season of *Strongylocentrotus purpuratus* (Stimpson). *Biol Bull*, 148, 393-401

Connell J.H. (1985) The consequences of variation in initial settlement vs. post-settlement mortality in rocky intertidal communities. *J Exp Mar Biol Ecol*, 93, 11-45

Davis R.E., Ohman M.D., Rudnick D.L. & Sherman J.T. (2008) Glider surveillance of physics and biology in the southern California Current System. *Limnol Oceanogr*, 53, 2151-2168

Di Lorenzo E., Schneider N., Cobb K.M., Franks P., Chhak K., Miller A.J., McWilliams J.C., Bograd S.J., Arango H. & Curchitser E. (2008) North Pacific Gyre Oscillation links ocean climate and ecosystem change. *Geophysical Research Letters*, 35

Di Lorenzo E., Combes V., Keister J.E., Strub P.T., Thomas A.C., Franks P.J., Ohman M.D., Furtado J.C., Bracco A. & Bograd S.J. (2013) Synthesis of Pacific Ocean climate and ecosystem dynamics. *Oceanography*, 26, 68-81

DiGiacomo P.M. & Holt B. (2001) Satellite observations of small coastal ocean eddies in the Southern California Bight. *Journal of Geophysical Research: Oceans*, 106, 22521-22543

Ebert T. (1983) Recruitment in echinoderms. *Echinoderm Stud*, 1, 169-203

Ebert T., Schroeter S., Dixon J. & Kalvass P. (1994) Settlement patterns of red and purple sea urchins (*Strongylocentrotus franciscanus* and *S. purpuratus*) in California, USA. *Mar Ecol Prog Ser*, 111, 41-52

Ebert T.A. (2010) Demographic patterns of the purple sea urchin *Strongylocentrotus purpuratus* along a latitudinal gradient, 1985-1987. *Mar Ecol Prog Ser*, 406, 105-120

Edmunds P.J. & Carpenter R.C. (2001) Recovery of Diadema antillarum reduces macroalgal cover and increases abundance of juvenile corals on a Caribbean reef. *Proceedings of the National Academy of Sciences*, 98, 5067-5071

Estes J.A. & Duggins D.O. (1995) Sea otters and kelp forests in Alaska: generality and variation in a community ecological paradigm. *Ecol Monogr*, 65, 75-100

Feehan C.J. & Scheibling R.E. (2014) Effects of sea urchin disease on coastal marine ecosystems. *Mar Biol*, 161, 1467-1485

Field C.M. & Walker C. 2003. *A Site Profile of the Kachemak Bay Research Reserve, a Unit of the National Estuarine Research Reserve System*. Kachemak Bay Research Reserve Homer

Filbee-Dexter K. & Scheibling R.E. (2014) Sea urchin barrens as alternative stable states of collapsed kelp ecosystems. *Mar Ecol Prog Ser*, 495, 1-25

Fisher J.L., Peterson W.T. & Morgan S.G. (2014) Does larval advection explain latitudinal differences in recruitment across upwelling regimes? *Mar Ecol Prog Ser*, 503, 123-137

Foster M.C., Byrnes J.E. & Reed D.C. (2015) Effects of five southern California macroalgal diets on consumption, growth, and gonad weight, in the purple sea urchin *Strongylocentrotus purpuratus*. *PeerJ*, 3, e719

Gilbert D. (1997) Towards a new recruitment paradigm for fish stocks. *Can J Fish Aquat Sci*, 54, 969-977

Gonor J.J. (1973) Reproductive cycles in oregon populations of the echlnoid, *StrongylocentrotUs purpuratus* (Stimpson). I. Annual gonad growth and ovarian gametogenic cycles. *J Exp Mar Biol Ecol*, 12, 45-64

Grosberg R.K. & Levitan D.R. (1992) For adults only? Supply-side ecology and the history of larval biology. *Trends Ecol Evol*, 7, 130-133

Harrold C. & Reed D.C. (1985) Food availability, sea urchin grazing, and kelp forest community structure. *Ecology*, 66, 1160-1169

Hernández J.C., Clemente S., Girard D., Pérez-Ruzafa Á. & Brito A. (2010) Effect of temperature on settlement and postsettlement survival in a barrens-forming sea urchin. *Mar Ecol Prog Ser*, 413, 69-80

Hoegh-Guldberg O. & Pearse J.S. (1995) Temperature, food availability, and the development of marine invertebrate larvae. *Am Zool*, 35, 415-425

Kato S. & Schroeter S.C. (1985) Biology of the red sea urchin, *Strongylocentrotus franciscanus*, and its fishery in California. *Mar. Fish. Rev*, 47, 1-20

Kushner D.J., Rassweiler A., McLaughlin J.P. & Lafferty K.D. (2013) A multi-decade time series of kelp forest community structure at the California Channel Islands: Ecological Archives E094-245. *Ecology*, 94, 2655-2655

Lafferty K.D. (2004) Fishing for lobsters indirectly increases epidemics in sea urchins. *Ecol Appl*, 14, 1566-1573

Ling S., Johnson C., Ridgway K., Hobday A. & Haddon M. (2009) Climate-driven range extension of a sea urchin: inferring future trends by analysis of recent population dynamics. *Global Change Biology*, 15, 719-731

Lynn R. & Bograd S. (2002) Dynamic evolution of the 1997–1999 El Niño–La Niña cycle in the southern California Current system. *Progress in Oceanography*, 54, 59-75

Magnusson A., Skaug H.J., Nielsen A., Berg C.W., Kristensen K., Maechler M., Bentham K.J.v., and B.M.B. & Brooks M.E. (2017) glmmTMB: Generalized Linear Mixed Models using Template Model Builder. R package version 0.1.3. Available at https://github.com/glmmTMB

Mantua N.J., Hare S.R., Zhang Y., Wallace J.M. & Francis R.C. (1997) A Pacific interdecadal climate oscillation with impacts on salmon production. *Bulletin of the american Meteorological Society*, 78, 1069-1080

Mantua N.J. & Hare S.R. (2002) The Pacific decadal oscillation. *Journal of Oceanography*, 58, 35-44

McManus M.A. & Woodson C.B. (2012) Plankton distribution and ocean dispersal. *J Exp Biol*, 215, 1008-1016

Menge B.A., Gouhier T.C., Freidenburg T. & Lubchenco J. (2011) Linking long-term, large-scale climatic and environmental variability to patterns of marine invertebrate recruitment: Toward explaining "unexplained" variation. *J Exp Mar Biol Ecol*, 400, 236-249

Menge B.A. & Menge D.N. (2013) Dynamics of coastal meta-ecosystems: the intermittent upwelling hypothesis and a test in rocky intertidal regions. *Ecol Monogr*, 83, 283-310

Mitarai S., Siegel D., Watson J., Dong C. & McWilliams J. (2009) Quantifying connectivity in the coastal ocean with application to the Southern California Bight. *J Geophys Res*, 114

Morgan S.G., Fisher J.L., Miller S.H., McAfee S.T. & Largier J.L. (2009) Nearshore larval retention in a region of strong upwelling and recruitment limitation. *Ecology*, 90, 3489-3502

Morgan S.G. (2014) Behaviorally mediated larval transport in upwelling systems. *Advances in Oceanography*, 2014

Morgan S.G., Shanks A.L., Fujimura A.G., Reniers A.J., MacMahan J., Griesemer C.D., Jarvis M. & Brown J. (2016) Surfzone hydrodynamics as a key determinant of spatial variation in rocky intertidal communities. *Proc R Soc B*, 283, 20161017

Morgan S.G.M., Miller S.H., Robart M.J. & Largier J.L. (2018) Nearshore larval retention and cross-shelf migration of benthic crustaceans at an upwelling center. *Frontiers in Marine Science*, 5, 161

Myers R.A. (1998) When do environment–recruitment correlations work? *Rev Fish Biol Fish*, 8, 285-305

Okamoto D.K. 2014. *The role of fluctuating food supply on recruitment, survival and population dynamics in the sea*. University of California, Santa Barbara

Okamoto D.K. (2016) Competition among eggs shifts to cooperation along a sperm supply gradient in an external fertilizer. *Am Nat*, 187, E129-E142

Olivares-Bañuelos N.C., Enríquez-Paredes L.M., Ladah L.B. & De La Rosa-Vélez J. (2008) Population structure of purple sea urchin Strongylocentrotus purpuratus along the Baja California peninsula. *Fisheries science*, 74, 804-812

Padilla-Gamiño J.L., Kelly M.W., Evans T.G. & Hofmann G.E. (2013) Temperature and CO2 additively regulate physiology, morphology and genomic responses of larval sea urchins, *Strongylocentrotus purpuratus*. *Proc R Soc B*, 280

Pearse J.S., Pearse V.B. & Davis K.K. (1986) Photoperiodic Regulation of Gametogenesis and Growth in the Sea Urchin *Strongylocentrotus purpuratus*. *J Exp Zool*, 237, 107-118

Pearse J.S. (2006) Ecological role of purple sea urchins. *Science*, 314, 940-941

Piironen J. & Vehtari A. (2017) Sparsity information and regularization in the horseshoe and other shrinkage priors. *Electronic Journal of Statistics*, 11, 5018-5051

Pineda J. (1994) Internal tidal bores in the nearshore: Warm-water fronts, seaward gravity currents and the onshore transport of neustonic larvae. *Journal of Marine Research*, 52, 427-458

Pineda J., Reyns N. & Lentz S.J. (2018) Reduced barnacle larval abundance and settlement in response to large-scale oceanic disturbances: Temporal patterns, nearshore thermal stratification, and potential mechanisms. *Limnol Oceanogr*, 63, 2618-2629

Reynolds R.W., Smith T.M., Liu C., Chelton D.B., Casey K.S. & Schlax M.G. (2007) Daily high-resolution-blended analyses for sea surface temperature. *J Clim*, 20, 5473-5496

Roughgarden J., Pennington J., Stoner D., Alexander S. & Miller K. (1991) Collisions of upwelling fronts with the intertidal zone: the cause of recruitment pulses in barnacle populations of central California. *Acta Oecol*, 12, 35-51

Rowley R. (1989) Settlement and recruitment of sea urchins (*Strongylocentrotus spp*.) in a sea-urchin barren ground and a kelp bed: are populations regulated by settlement or post-settlement processes? *Mar Biol*, 100, 485-494

Runcie D.E., Garfield D.A., Babbitt C.C., Wygoda J.A., Mukherjee S. & Wray G.A. (2012) Genetics of gene expression responses to temperature stress in a sea urchin gene network. *Mol Ecol*, 21, 4547-4562

Sathyendranath S., Grant M., Brewin R.J.W., Brockmann C., Brotas V., Chuprin A., Doerffer R., Dowell M., Farman A., Groom S., Jackson T., Krasemann H., Lavender S., Martinez Vicente V., Mazeran C., Mélin F., Moore T.S., Müller D., Platt T., Regner P., Roy S., Steinmetz F., Swinton J., Valente A., Zühlke M., Antoine D., Arnone R., Balch W.M., Barker K., Barlow R., Bélanger S., Berthon J.-F., Beşiktepe Ş., Brando V.E., Canuti E., Chavez F., Claustre H., Crout R., Feldman G., Franz B., Frouin R., García-Soto C., Gibb S.W., Gould R., Hooker S., Kahru M., Klein H., Kratzer S., Loisel H., McKee D., Mitchell B.G., Moisan T., Muller-Karger F., O'Dowd L., Ondrusek M., Poulton A.J., Repecaud M., Smyth T., Sosik H.M., Taberner M., Twardowski M., Voss K., Werdell J., Wernand M. & Zibordi G. (2018) ESA Ocean Colour Climate Change Initiative (Ocean_Colour_cci): Version 3.1 Data. Centre for Environmental Data Analysis. http://dx.doi.org/10.5285/9c334fbe6d424a708cf3c4cf0c6a53f5

Schroeder T. & Battaglia D. (1985) "Spiral asters" and cytoplasmic rotation in sea urchin eggs: induction in *Strongylocentrotus purpuratus* eggs by elevated temperature. *J Cell Biol*, 100, 1056-1062

Shanks A. & Shearman R. (2009) Paradigm lost? Cross-shelf distributions of intertidal invertebrate larvae are unaffected by upwelling or downwelling. *Mar Ecol Prog Ser*, 385, 189-204

Shanks A.L. (1983) Surface slicks associated with tidally forced internal waves may transport pelagic larvae of benthic invertebrates and fishes shoreward. *Marine ecology progress series. Oldendorf*, 13, 311-315

Shanks A.L. & Eckert G.L. (2005) Population persistence of California Current fishes and benthic crustaceans: a marine drift paradox. *Ecol Monogr*, 75, 505-524

Shanks A.L. (2009) Pelagic larval duration and dispersal distance revisited. *The Biological Bulletin*, 216, 373-385

Shanks A.L., Morgan S.G., MacMahan J. & Reniers A.J. (2017) Alongshore variation in barnacle populations is determined by surf zone hydrodynamics. *Ecol Monogr*, 87, 508-532

Shanks A.L. & Morgan S.G. (2018) Testing the intermittent upwelling hypothesis: upwelling, downwelling, and subsidies to the intertidal zone. *Ecol Monogr*, 88, 22-35

Shelton A.O. & Mangel M. (2011) Fluctuations of fish populations and the magnifying effects of fishing. *Proceedings of the National Academy of Sciences*, 108, 7075-7080

Shkedy Y. & Roughgarden J. (1997) Barnacle recruitment and population dynamics predicted from coastal upwelling. *Oikos*, 487-498

765 Siegel D., Kinlan B., Gaylord B. & Gaines S. (2003) Lagrangian descriptions of marine larval
766 dispersion. *Mar Ecol Prog Ser*, 260, 83-96
767 Siegel D., Mitarai S., Costello C., Gaines S., Kendall B., Warner R. & Winters K. (2008) The
768 stochastic nature of larval connectivity among nearshore marine populations.
769 *Proceedings of the National Academy of Sciences*, 105, 8974-8979
770 Strathmann M.F. 1987. *Reproduction and development of marine invertebrates of the northern*
771 *Pacific coast: data and methods for the study of eggs, embryos, and larvae*. Univ. of
772 Wash. Press, Seattle
773 Strathmann R. (1978) Length of pelagic period in echinoderms with feeding larvae from the
774 northeast Pacific. *J Exp Mar Biol Ecol*, 34, 23-27
775 Sydeman W.J., Poloczanska E., Reed T.E. & Thompson S.A. (2015) Climate change and marine
776 vertebrates. *Science*, 350, 772-777
777 Szuwalski C.S., Vert-Pre K.A., Punt A.E., Branch T.A. & Hilborn R. (2015) Examining common
778 assumptions about recruitment: a meta-analysis of recruitment dynamics for worldwide
779 marine fisheries. *Fish and Fisheries*, 16, 633-648
780 Tegner M. & Dayton P. (1991) Sea urchins, El Niños, and the long term stability of Southern
781 California kelp forest communities. *Mar Ecol Prog Ser*, 77, 49-63
782 Thorson J.T., Skaug H.J., Kristensen K., Shelton A.O., Ward E.J., Harms J.H. & Benante J.A.
783 (2015) The importance of spatial models for estimating the strength of density
784 dependence. *Ecology*, 96, 1202-1212
785 Underwood A. & Fairweather P. (1989) Supply-side ecology and benthic marine assemblages.
786 *Trends Ecol Evol*, 4, 16-20

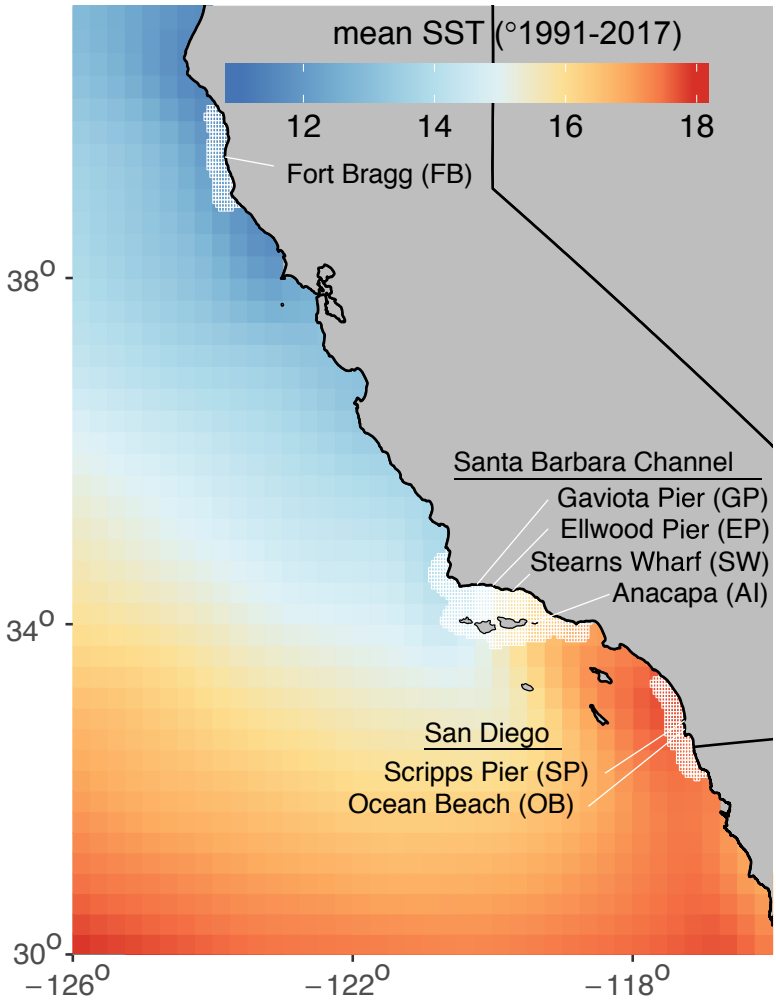

Figure 1: Map of larval settlement collection sites in California. Colors represent the average spatial gradient of sea surface temperature from 1991-2017. The hatched white lines show the shoreline buffer used to constrain sea surface temperature and sea surface chlorophyll index to local larval settlement observations.

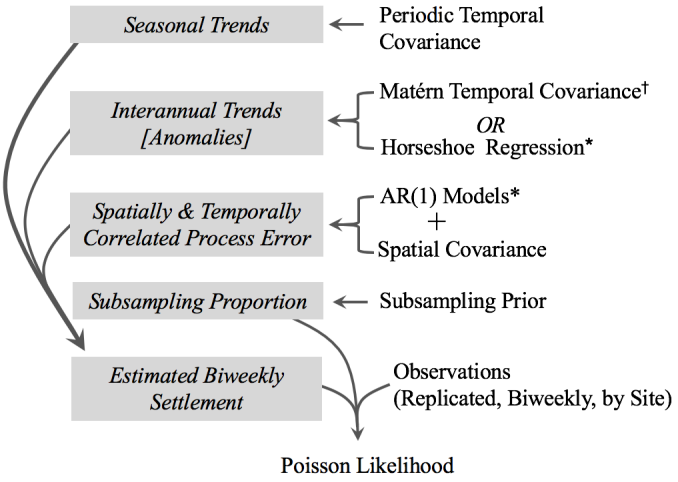

Figure 2: Diagram of the model structure using either a Matérn temporal covariance (trend estimation model) or a horseshoe regression (correlation estimation model) to estimate seasonal anomalies. For details see Tables 1 and 2. *Bayesian Regression Model Only. † Trend Estimation Model Only

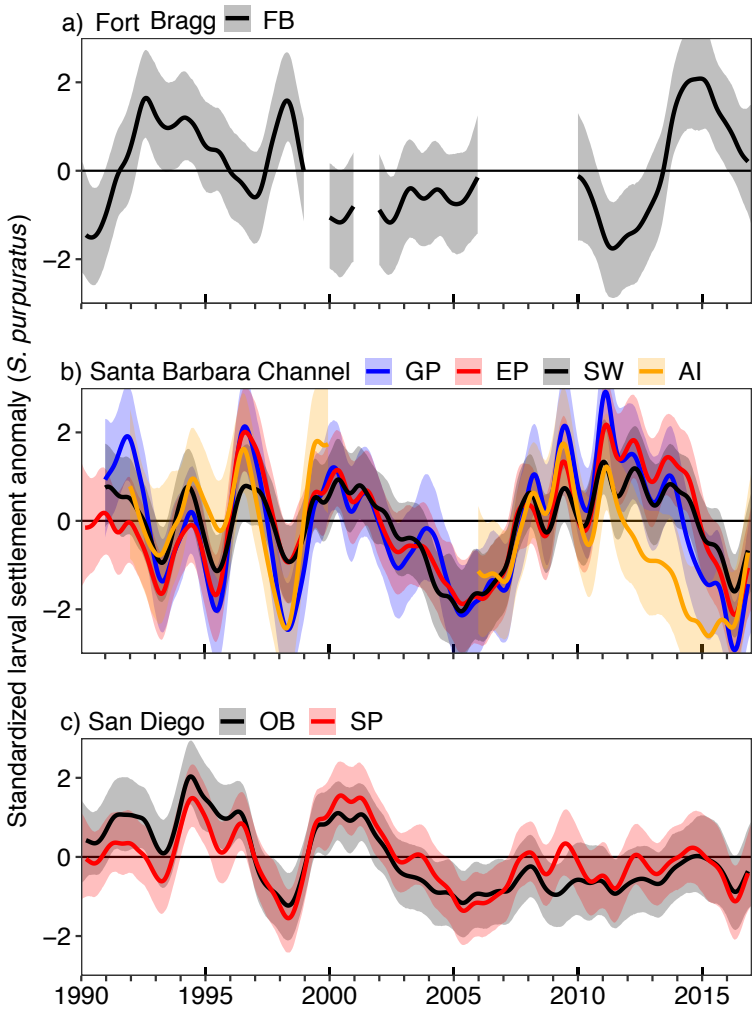

Figure 3: Standardized annual scale trends (log-scale, standardized to one SD) of larval settlement S. purpuratus from 1990 through 2016 for: (a) Fort Bragg, (b) sites in the Santa Barbara Channel, and (c) sites in San Diego. Colors within represent individual sites associated with the legend. Interannual trends are estimated using a 3/2 Matrn Gaussian process covariance within a Bayesian multivariate state-space model accounting for spatiotemporal correlations.

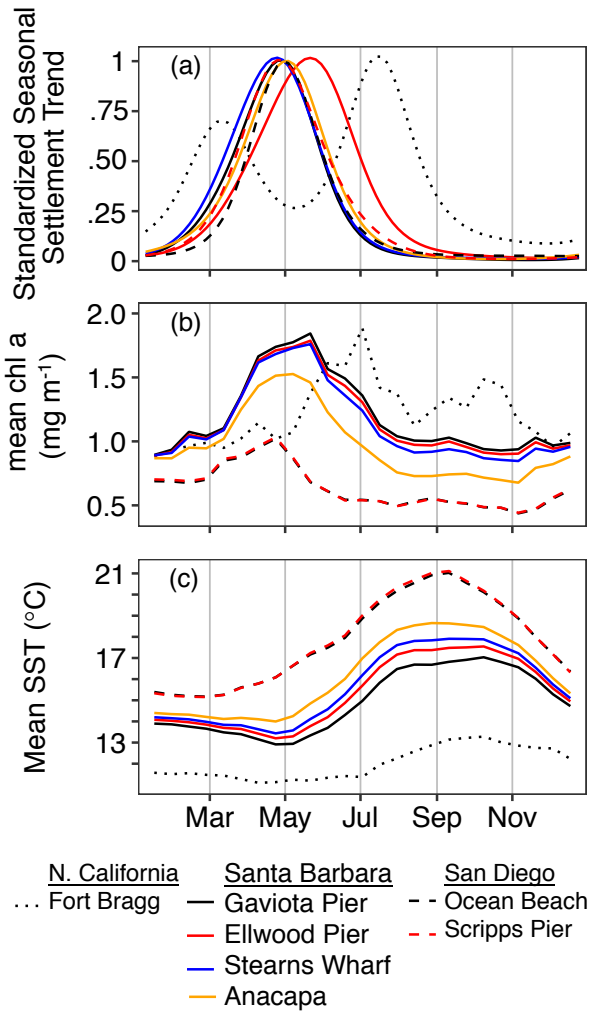

Figure 4: Seasonal trends at each site for: (a) standardized larval settlement of S. purpuratus, (b) biweekly mean sea surface chlorophyll a (chl a) and (c) biweekly mean sea surface temperature (SST). The seasonal trend in larval settlement at each site was standardized by the mean maximum seasonal value. Chl a and SST were measured using satellite imagery within 25 km of the coastline and 150 alongshore km of the location where settlement was sampled (hatched areas in Figure 1). See Methods for details.

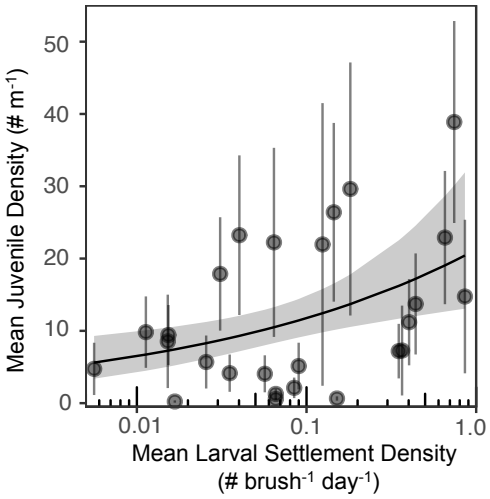

Figure 5: The relationship between the summer density of juvenile purple sea urchins on reefs in the Santa Barbara Channel and the density of recruits on larval collectors during March- July of the previous year (i.e., 12-20 months prior). Points and error bars represent annual means (+/- SE) averaged over all sites. The line with the band represents the estimated relationship and 95% uncertainty interval.

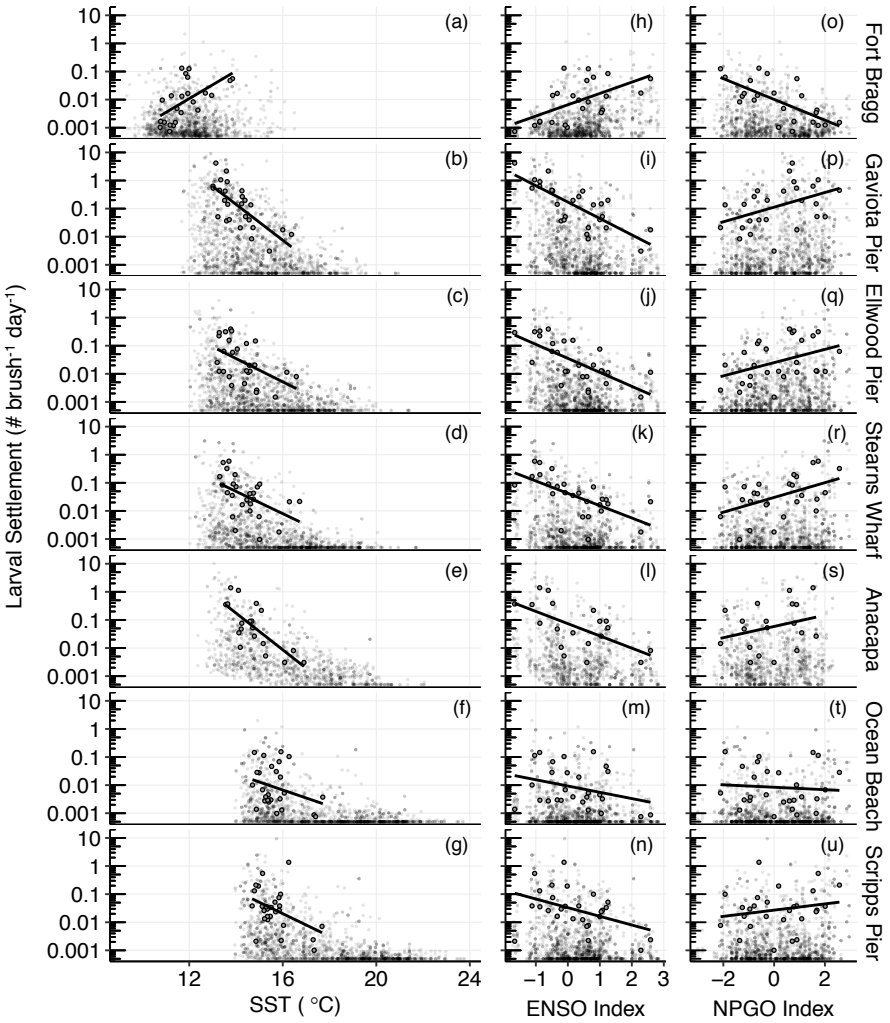

Figure 6: Relationships between larval settlement of purple sea urchins at each site and: (a-g) sea surface temperature, (h-n) the multivariate ENSO index, and (m-u) the North Pacific Gyre Oscillation (NPGO). Small grey points represent biweekly means and black points and lines represent annual means.

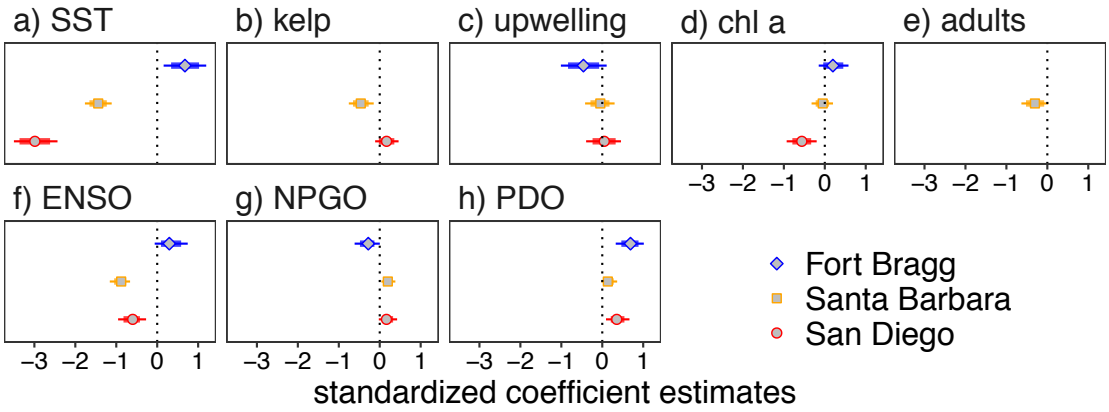

Figure 7: Standardized Bayesian multiple regression coefficients for relationships between *S. purpuratus* settlement and local covariates (a-e) or global climatic indices (f-h). Models with global and local variables were fit separately. Coefficients were estimated using a multiple regression nested within a Bayesian multivariate time series model. Coefficients are a priori biased towards zero using a regularized horseshoe prior for variable selection. For details see Methods, Figure 2 and appendix for details.

Table 1: Equations for the multivariate spatiotemporal models. Variables, parameters and priors are described in Table 2. Note that there are two primary model forms: a trend estimation model, and a Bayesian regression model. Equations apply to both model forms except where specified.

Eq.	**Description**	**Equation**
3	total count likelihood	$\begin{cases} Tot_{t,s,b} \sim \text{Poisson}(\hat{\mu}_{t,s} \times D_{t,s,b}/p_{t,s,b}) & \text{when subsampled} \\ N_{t,s,b} \sim \text{Poisson}(\hat{\mu}_{t,s} \times D_{t,s,b}) & \text{otherwise} \end{cases}$
4	subsampling prior	$p_{t,s,b} \sim \text{beta}(N_{t,s,b} + 0.5, NO_{t,s,b} + 0.5)$ when subsampled
5	prior seasonal temporal correlation function	$\bar{r}_{<t_i,t_j>} = \exp\left[-\frac{2}{1.5^2}(0.5 - 0.5\cos(\pi\lvert t_i - t_j\rvert))\right]$ Periodic Kernel (MacKay 1998)
6†	prior annual temporal correlation function	$\bar{\bar{r}}_{<t_i,t_j>} = (1 + 3^2\lvert t_i - t_j\rvert)e^{-3^2\lvert t_i - t_j\rvert}$ Matérn 3/2 Kernel (Rasmussen & Williams 2006)
7	prior seasonal spatiotemporal covariance function (separable)	$\bar{\boldsymbol{\Sigma}} = \bar{\boldsymbol{\Omega}} \otimes [\bar{\boldsymbol{\sigma}}\bar{\boldsymbol{R}}]$
8†	prior annual spatiotemporal covariance function (separable)	$\bar{\bar{\boldsymbol{\Sigma}}} = \bar{\bar{\boldsymbol{\Omega}}} \otimes [\bar{\bar{\boldsymbol{\sigma}}}\bar{\bar{\boldsymbol{R}}}]$
9	matrix of seasonal trends	$\textbf{Seasonal} \sim \text{MVN}(0, \bar{\boldsymbol{\Sigma}})$
10†	matrix of annual trends	$\textbf{Annual} \sim \text{MVN}(0, \bar{\bar{\boldsymbol{\Sigma}}})$
11a*	first order autoregressive model	$\boldsymbol{\epsilon}_t = \boldsymbol{\phi}\boldsymbol{\epsilon}_{t-1} + \boldsymbol{e}_t\sqrt{(1 - \boldsymbol{\phi}^2)}$
11b	spatially correlated process error	$\boldsymbol{e}_t \sim \text{MVN}(0, \boldsymbol{\sigma}\boldsymbol{\Omega})$

∗ Bayesian Regression Model Only
† Trend Estimation Model Only

Table 2: Definition of parameters, variables, and priors for equations described in Table 1

Symbol	**Description**	**Type**	Prior/Input
$\hat{\mu}_{t,s}$	expected settlement density (per brush, per day) of purple urchins, defined in Eqs. 1 or 2 in the main text for each model.	estimated	Eqs. 1, 2
$N_{t,s,b}$	number of purple urchins counted at time t, site s and brush b. When urchin species within brushes are subsampled, data produced are a total urchin count ($Tot_{t,s,b}$), a total subsample count ($NO_{t,s,b}$, and a purple urchin subsample count ($N_{t,s,b}$).	input	data
$Tot_{t,s,b}$	total number of urchins counted at time t, site s and brush b	input	data
$p_{t,s,b}$	estimated proportion of purple urchins in the counts given the subsample (when urchin counts in brushes are subsampled).	input	data
$D_{t,s,b}$	exact number of days of the brush deployment	input	data
$\mathbf{X}$	covariate design matrix - for estimation model represents only site indices, for regression model includes covariates	input	data
$\boldsymbol{\beta}$	vector of site specific scale parameters and covariate coefficients	estimated	**Scale parameters**: Student-t: scale=2; **Coefficients**: regularized horseshoe prior (see methods).
$\boldsymbol{\phi}$	vector of site specific first order autoregressive parameters & estimated (regression model only)	estimated	Uniform -0.95 to 0.95
$\boldsymbol{\Omega}, \bar{\boldsymbol{\Omega}}, \bar{\bar{\boldsymbol{\Omega}}}$	spatial correlation matrices for process error, annual trends, and seasonal trends (estimated through the cholesky factor)	estimated	LKJ prior:scale= 2 (Lewandowski *et al.* 2009)
$\bar{\boldsymbol{R}}, \bar{\bar{\boldsymbol{R}}}$	temporal correlation matrices for annual and seasonal gaussian processes	input	eqs 5 & 6
$\boldsymbol{\sigma}$, $\bar{\boldsymbol{\sigma}}$, $\bar{\bar{\boldsymbol{\sigma}}}$	site specific standard deviation for process error, annual trends, and seasonal trends	estimated	half-Cauchy: scale = 2.5 (Polson & Scott 2012)

Supplementary Information - Appendices for "Geographically Opposing Responses of Sea Urchin Recruitment to Changes in Ocean Climate"

Daniel K. Okamoto*[1,2], Stephen Schroeter†[3], and Daniel C. Reed‡[3]

[1]Department of Biological Science, Florida State University, Tallahassee, Florida 32303
[2]Ecology, Evolution and Marine Biology, University of California Santa Barbara, Santa Barbara, CA 93106 USA
[3]Marine Science Institute, University of California Santa Barbara, Santa Barbara, CA 93106 USA

*corresponding author: dokamoto@bio.fsu.edu
†email: schroete@lifesci.ucsb.edu
‡email: dan.reed@lifesci.ucsb.edu
*corresponding author: dokamoto@bio.fsu.edu
†email: schroete@lifesci.ucsb.edu
‡email: dan.reed@lifesci.ucsb.edu

Estimation of juvenile urchin densities

The KFM program surveys purple sea urchins at the Santa Barbara Channel Islands by counting the total number of individuals in defined areas and measuring approximately 100 individuals at each site. Thus, to model density we used the number of juveniles measured divided by the total number of individuals measured, multiplied by the total number of individuals counted, divided by the area surveyed:

$$Juvenile \quad Density_{i,t} = \frac{Juveniles \quad Measured_{i,t}}{Total \quad Measured_{i,t}} \frac{Total \quad Count_{i,t}}{Total \quad Area_{i,t}}$$

We modeled density in the GLM using the number of measured juvenile urchins (2.5 cm in test diameter- the approximate cutoff size for reproduction - Kenner & Lares 1991). Let represent expected juvenile density at site i in year t. We constructed the regression as:

$$\ln\mu_{i,t} = \alpha_i + \beta \quad \ln Larval \quad recruitment_t$$

We allowed the intercept (α_i) to vary by site nested within each island because of overall differences in mean juvenile density among sites and islands. We used a negative binomial (NB) with the using direct mean and variance parameterization form:

$$Juveniles \quad Measured_{i,t} \sim \mathrm{NB}(\ln\mu_{i,t} - \ln[\frac{1}{TotalMeasured_{i,t}} \frac{TotalCounted_{i,t}}{TotalArea_{i,t}}], \sigma^2)$$

We constructed the model in this format (i.e. with the density denominator in the left hand side of the equation) to maintain the sample size and integer nature of the data while modeling the mean density.

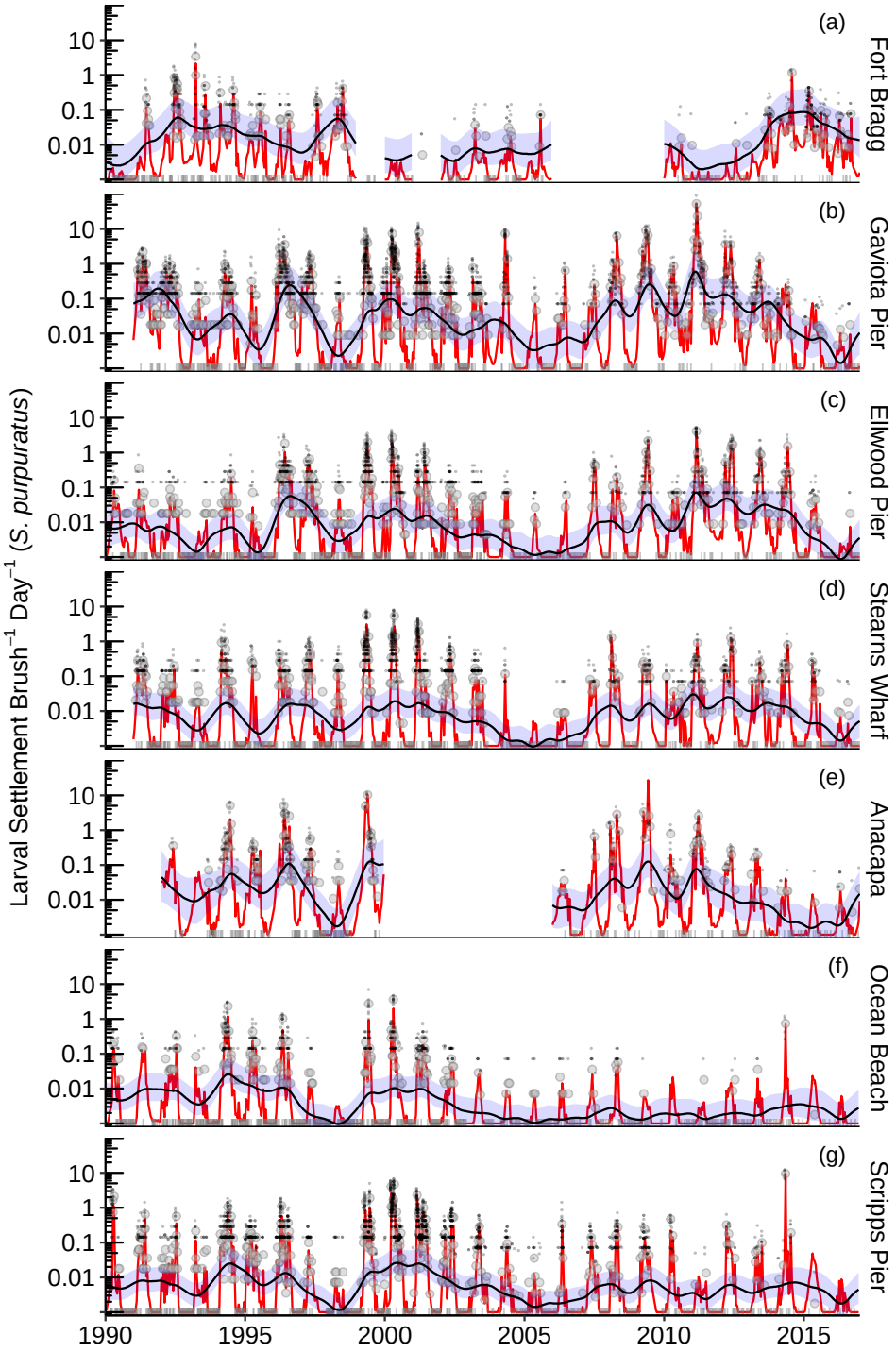

Figure S.1: Observed and estimated purple urchin (*S. purpuratus*) settlement trends from 1990-2016 for each site. Large points represent empirical biweekly means (non-zero means across all brushes and collection times), lines on the axis represent biweekly mean values equal to zero, small points represent counts on individual brushes (non-zero only), red lines represent biweekly estimates, lines with blue 95% uncertainty intervals represent model estimates of the interannual trends. The model estimates the seasonal trend and the interannual trend at each site simultaneously. For reference, interannual trends for *S. purpuratus* shown here are the unstandardized versions of those shown in Figure 2.

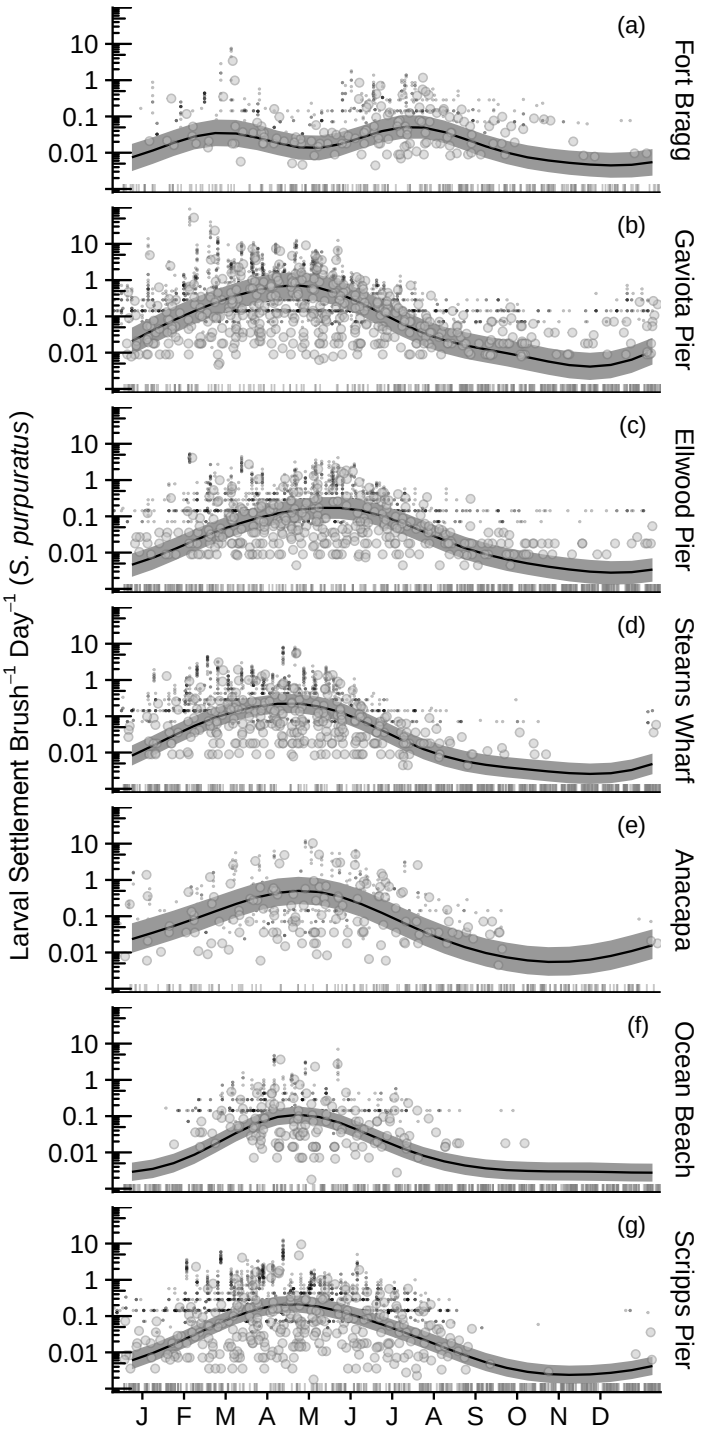

Figure S.2: Seasonal settlement trends from 1990-2016 with the mean estimated seasonal trend for each site. Large points represent empirical biweekly means (non-zero means across all brushes and collection times), lines on the axis represent biweekly mean values equal to zero, small points represent counts on individual brushes (non-zero only), black lines represent the posterior mean and bands represent the 95% uncertainty interval. The model estimates the seasonal trend and the interannual trend at each site simultaneously. For reference, seasonal trends for *S. purpuratus* shown here are the unstandardized versions of those shown in Figure 3.

Variable Correlations

To illustrate the intercorrelated nature of the covariates and responses, we estimated a network model for Gaviota Pier that includes the independent model estimates of *S. purpuratus* settlement and its seasonality. To do so, we first constrained network structure by excluding all nonsensical interactions (i.e. chlorophyll does not cause ENSO events and is thus eliminated a priori) and including all known directional interactions (i.e. estimated seasonality affecting settlement for is forced into the network). Learning of the network skeleton is achieved via the Hill Climbing algorithm using the bnlearn (Scutari 2010) package in R. Note that strong collinearity can result in the weaker correlation being ignored (e.g. ENSO over SST with Larval Recruitment).

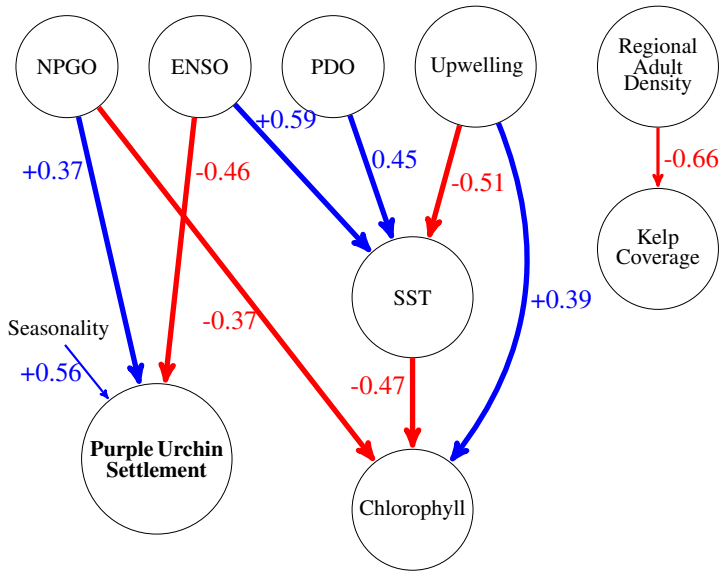

Figure S.3: Bayesian network model structure inferred for the Santa Barbara Channel. Numbers represent the partial correlation coefficients accounting for all other variables pointing to that node. All correlations shown are significant at alpha= 0.05

References

Kenner M. & Lares M. (1991) Size at first reproduction of the sea urchin *Strongylocentrotus purpuratus* in a central California kelp forest. Mar Ecol Prog Ser, 76, 303-306

Lewandowski D., Kurowicka D. & Joe H. (2009) Generating random correlation matrices based on vines and extended onion method. J Multivar Anal, 100, 1989-2001

MacKay D.J. (1998) Introduction to Gaussian processes. NATO ASI Series F Computer and Systems Sciences, 168, 133-166

Polson N.G. & Scott J.G. (2012) On the half-Cauchy prior for a global scale parameter. Bayesian Analysis, 7, 887-902

Rasmussen C.E. & Williams C.K.I. 2006. Gaussian Processes for Machine Learning. The MIT Press, Cambridge, Massachusetts

Scutari M. (2010). Learning Bayesian Networks with the bnlearn R Package. Journal of Statistical Software, 35(3), 1-22. URL http://www.jstatsoft.org/v35/i03/

```
\\\
```

```
  vector[NO] S_exp; // normal scale estimated sp for each observation

  vector[NO] theta2; // fraction that is SP

  matrix[NM,NS] w;

  // correlated errors
  matrix[NM,NS] e;

  LS  = D_seas*z_s;
  w = D_ann*transpose(L_Omega_Spatial*w_z);

  theta2 = rep_vector(1.0,NO);
  theta2[SUB] = theta;
  // put it all together
  e = transpose(diag_pre_multiply(sigma_S_mu,L_Omega_S)*e_z);
  S= rep_matrix(mu_S,NM)+diag_post_multiply(LS[PRED_MONTH,],sigma2)+
      diag_post_multiply(w,sigma)+e;
  S_exp = exp(to_vector(S)[OBS]) .*D ./theta2;
}

model {
  sigma ~ cauchy(0, 0.5);
  sigma2 ~ cauchy(0, 0.5);

  L_Omega_S ~ lkj_corr_cholesky(2);
  L_Omega_Spatial ~ lkj_corr_cholesky(2);

  for(i in 1:NS){
    z_s[i]~ normal(0,1);
    mu_S[i] ~ normal(0,5);
  }

  sigma_S_mu ~ cauchy(0,2.5);

  // uncertainty on proportions of purples in the sample
  // jeffrey's prior given subsampling
  theta~beta(P1, P2);

  // observation likelihood
  N~poisson(S_exp);
}
```

```
\\\
```

```
  // iid errors for seasonal gaussian process
  vector[NP] beta_tilde;
  vector<lower=0>[NP] lambda;
  real<lower=0> c2_tilde;
  real<lower=0> tau_tilde;
  real alpha;
}

transformed parameters {
  matrix[NYM,NS] LS; // log scale expected sp per brush, per day for every month
  matrix[NM,NS] S; // estimated abundance
  vector[NO] S_exp; // normal scale estimated sp for each observation

  vector[NO] N_mu; // expected total count
  vector[NO] q_mu; // expected fraction of N that is SP
  vector[NS] sigma_star;

  vector[NM*NS] s_hat;

  // process variables
  vector[NO] theta2; // fraction that is SP

  // correlated errors
  matrix[NM,NS] e;
  matrix[NM,NS] e_hat;

  vector[NP] beta;
  vector[NP] lambda_tilde;

  real tau0 = (m0/(NP-m0))*(mean(sigma_S_mu)*sqrt(1.0*NM*NS));
  real slab_scale2 = square(slab_scale);
  real half_slab_df = 0.5 * 25;

  real tau = tau0 * tau_tilde;
  real c2 = slab_scale2 * c2_tilde;
  lambda_tilde  = sqrt( c2 * square(lambda) ./ (c2 + square(tau) * square(lambda))
      );
  beta = tau * lambda_tilde .* beta_tilde;

  // regression model
  s_hat = X*beta;

  // seasonal gaussian process model
  LS  = D_seas*z_s;

  // process error
  for(i in 1:NS){
    sigma_star[i] = sigma_S_mu[i]*sqrt(1.0-phi[i]^2.0);
  }
  e = transpose(diag_pre_multiply(sigma_star,L_Omega_S)*e_z);
  // put it all together

  for(j in 1:NS){
    e_hat[1,j] = e[1,j];
    S[1,j]=mu_S[j]+LS[PRED_MONTH[1],j]*sigma[j]+s_hat[xind[1,j]]+e_hat[1,j]-5;
    for(i in 2:NM){
      e_hat[i,j] =  phi[j]*e_hat[i-1,j]+e[i,j];
      S[i,j]=mu_S[j]+LS[PRED_MONTH[i],j]*sigma[j]+s_hat[xind[i,j]]+e_hat[i,j]-5;
```

```
    }
  }

  theta2 = rep_vector(1.0,NO);
  theta2[SUB] = theta[ID[SUB]];

  S_exp = exp(to_vector(S)[OBS]) .*D ./theta2;
}

model {
  sigma ~ normal(0.0, 2);

  L_Omega_S ~ lkj_corr_cholesky(2.0);

  for(i in 1:NS){
    z_s[i]~ normal(0.0,1.0);
    e_z[i]~ normal(0.0,1.0);
    mu_S[i] ~ cauchy(0.0,10);
  }

  sigma_S_mu ~ normal(0.0,sigma_scale);

  beta_tilde ~ normal(0, 1);
  lambda ~ cauchy(0, 1);
  tau_tilde ~ cauchy(0, 1);
  c2_tilde ~ inv_gamma(half_slab_df, half_slab_df);

  // jeffrey's prior given subsampling
  theta~beta(P1, P2);

  // observation likelihood
  N~poisson(S_exp);
}
```